Proceedings of the ASME 2010 3rd Joint US-European Fluids Engineering Summer Meeting and 8th International Conference on Nanochannels, Microchannels, and Minichannels
FEDSM-ICNMM2010
August 1-5, 2010, Montreal, Canada

FEDSM-ICNMM2010-30754

NUMERICAL MULTIPHYSICS MODELING OF MICRODROPLET MOTION DYNAMICS IN DIGITAL MICROFLUIDIC SYSTEMS

Ali Ahmadi
University of British Columbia
Kelowna, BC, Canada

Jonathan F. Holzman
University of British Columbia
Kelowna, BC, Canada

Homayoun Najjaran
University of British Columbia
Kelowna, BC, Canada

Mina Hoorfar
University of British Columbia
Kelowna, BC, Canada

ABSTRACT

In this paper a novel numerical algorithm is proposed for modeling the transient motion of microdroplets in digital microfluidic systems. The new methodology combines the effects of the electrostatic and hydrodynamic pressures to calculate the actuating and opposing forces and the moving boundary of the microdroplet. The proposed model successfully predicts transient motion of the microdroplet in digital microfluidic systems, which is crucial in the design, control and fabrication of such devices. The results of such an analysis are in agreement with the expected trend.

INTRODUCTION

One of the newest generations of the microfluidic systems is digital microfluidic devices which are based on the transport of discrete microdroplets on arrays of electrodes [1-3]. Such digital microfluidic devices offer high levels of scalability and reconfigurability [4]. Among numerous actuation methods proposed for moving the microdroplet on the electrodes, electrowetting [1, 3, 5, 6] has been extensively used due to its precise localization and control.

Modeling of digital microfluidic systems is crucial for design, control and fabrication processes [7-11]. However, the development of such models is not trivial since many complex physicochemical phenomena are involved simultaneously. The electrowetting force acts on the droplet as the actuating force, and there also exist opposing forces, such as three-phase contact line, shear and drag forces, acting on the microdroplet in the opposite direction to the motion. Moreover, it has been shown that a threshold voltage exists, below which the microdroplet cannot start its motion [12].

In this paper, a comprehensive multiphysics model is developed to predict transport dynamics of a variety of microdroplets in contemporary digital microfluidic systems. Electrohydrodynamic governing equations are solved to obtain the electric field, free surface charge distribution and electrostatic pressure. These values are then used in a numerical energy analysis to calculate actuation and opposing forces. The effects of electrostatic and hydrodynamic pressures on the motion and shape of the microdroplet are considered simultaneously [9, 13]. Although electrohydrodynamic forces are not a function of the microdroplet shape [14], these forces change the shape of the microdroplet via pressure distribution changes inside the microdroplet. This change in the shape of the microdroplet changes the force balance, as all the opposing forces depend on the shape. With this in mind, this work calculates all constituent forces in a multiphysics model by coupling electrostatic and hydrodynamic governing equations. The result of such an analysis is an accurate estimation of the actuation and opposing forces as well as the shape of the microdroplet. This ultimately results in the accurate prediction of the microdroplet dynamics.

THEORY

In order to have an accurate model of microdroplet motion, all the actuating and opposing forces have to be realistically estimated. The governing equation of the transient motion of the microdroplet can be written as

$$m\frac{\mathrm{d}^2x}{\mathrm{d}t^2} = F_{\mathrm{act}} - F_{\mathrm{w}} - F_{\mathrm{d}} - F_{\mathrm{cl}}\,, \qquad (1)$$

where m is the mass of the microdroplet, d^2x/dt^2 is the microdroplet acceleration, and F_{act}, F_w, F_d and F_{cl} are the actuation, shear, filler and three-phase contact line forces. Accurate estimation of different forces was studied and discussed before [8, 10, 11]. The main focus of this paper is the accurate implementation of the boundary conditions for microdroplet and coupling of the effects of the electrostatic and hydrodynamic pressures.

A microdroplet in a digital microfluidic system is shown in Figure 1. As can be seen, there are different regions: microdroplet (region 1), filler (region 2) and dielectric layers (region 3). It has been shown before that, in order to have an accurate estimation of the opposing forces, the shape of the microdroplet must be calculated precisely [10]. The electrostatic field outside the microdroplet and the viscosity inside the microdroplet are two main sources of the change of this microdroplet shape. While each effect has been considered separately in the past [10, 15], this paper offers a new methodology for coupling the effects of electrostatics and hydrodynamics.

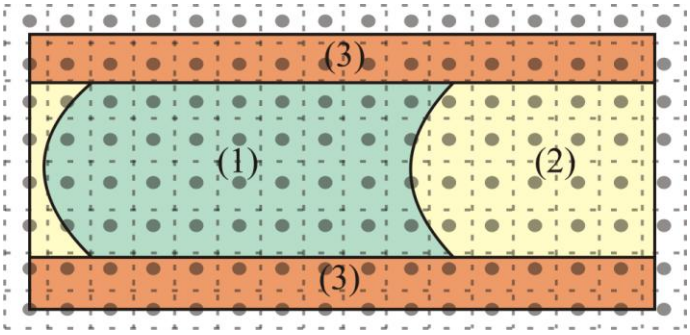

Figure 1. Different regions of a digital microfluidic system are shown: microdroplet (region 1), filler (region 2) and dielectric layers (region 3). Dashed lines show the Finite Volumes used for numerical solution. Black circles show the center of each cell.

The electrostatic pressure, hydrodynamic pressure and curvature of the surface are related as

$$[[p_{el}]]n_i - [[p_{hyd}]]n_i = \gamma(\nabla \bullet \vec{n})n_i, \qquad (2)$$

where $[[p_{hyd}]]$ and $[[p_{el}]]$ are the respective hydrodynamic and electrostatic pressure changes across the microdroplet interface with the filler, n_i is the i^{th} component of the unit vector, $\vec{n}$, normal to the interface, and γ is the liquid-vapor surface tension. As can be seen in equation (2), for the accurate estimation of the curvature (shape) of the interface, both the electrostatic pressure and the hydrodynamic pressure must be calculated. The hydrodynamic pressure as presented before [10, 16] can be calculated by solving the Navier-Stokes and continuity equations inside the microdroplet. On the other hand, the electrostatic pressure can be calculated by finding the electric potential and electric field outside the microdroplet as

$$p_{el} = \frac{1}{2}\varepsilon E^2, \qquad (3)$$

where ε is the permittivity of the filler and E is the electric field at the interface. The electric field is obtained from solving the Maxwell equation,

$$\vec{\nabla} \bullet \vec{D} = \vec{\nabla} \bullet (\varepsilon \vec{E}) = \vec{\nabla} \bullet (-\varepsilon \vec{\nabla}\Phi) = 0, \qquad (4)$$

where $\vec{D}$ is the electric displacement field. The equation (4), as shown in Figure 2, is written in discrete form for the cell (i,j) as

$$-D_{y,(i,j-1/2)} + D_{x,(i+1/2,j)} + D_{y,(i,j+1/2)} - D_{x,(i-1/2,j)} = 0 \qquad (5)$$

where D_x and D_y are the x– and y–components of the electric displacement which have to be calculated at the boundaries of the cell as shown in Figure 2. A Finite Volume Method is proposed for the numerical solution of the above equation. Details of the proposed Finite Volume Method are beyond the scope of this paper.

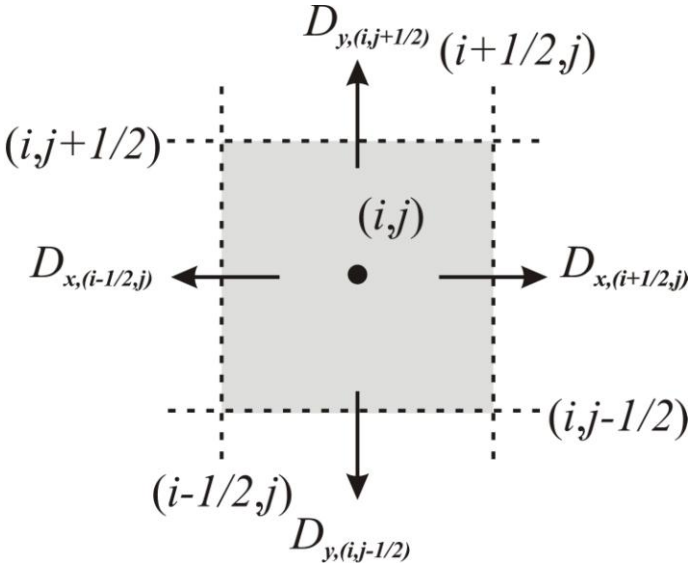

Figure 2. An arbitrary Finite Volume cell is shown.

Finally, after finding the electrostatic and hydrodynamic pressures, the curvature (shape) of the microdroplet is found using equation (2) [10].

In the proposed algorithm, at each time step, the electrostatic and hydrodynamic pressures, and hence the shape of the microdroplet for the next time step are calculated. Knowing the new shape, all the actuation and opposing forces are calculated accurately, and equation (1) is now solved to find the transient velocity of the microdroplet. Finally, the transient velocity is used in the Volume Of Fluid (VOF) method in order to model the moving boundary of the microdroplet. The algorithm used for solving equation (1) is shown in Figure 3.

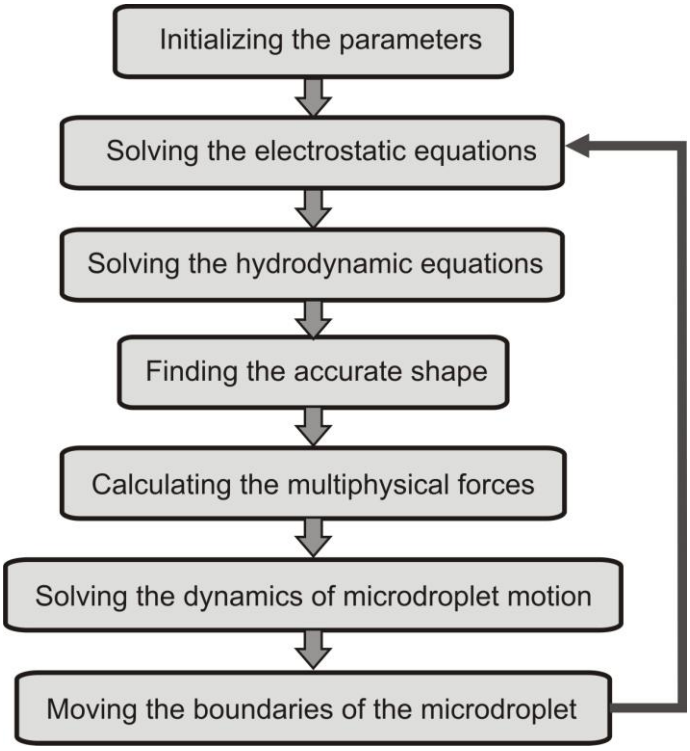

Figure 3: A flowchart of the proposed numerical algorithm is shown.

RESULTS AND DISCUSSION

The results of the proposed electrohydrodynamic analysis are shown in this section. The experimental setup introduced by Pollack et al. [17] is used here. An 800-nm-thick film of parylene C provided insulation over the control electrodes, and both the top and bottom plates had a 60-nm-thick top-coating of Teflon AF 1600. The filler fluid is 1 cSt Silicone oil. Dynamics of a 900 nL droplet of the 0.1 M KCl solution with an electrode pitch L = 1.5 mm, gap spacing h = 0.3 mm and droplet diameter d = 1.5 mm is modeled here.

Solutions of the hydrodynamics (inside) and electrostatics (outside) of the microdroplet for four different situations are shown in Figure 4. Figure 4a shows the system under the condition of no applied voltage for which all the contact angles are 105^o (i.e. the contact angle value of the solution with Teflon). Figures 4b, 4c and 4d show the moving microdroplet in three different positions (i.e. x = 0.3 mm, 0.75 mm, and 1.5 mm, respectively). The actuation voltage is 50 V. As can be seen here, vortices form inside the microdroplet due to its motion [10]. Also, the electric potential distribution outside the microdroplet is shown. Since the modeled microdroplet is a conductive liquid (0.1 M KCl) it is an iso-potential volume. However, the voltage of the microdroplet is a function of its position as shown in Figure 5. The voltage of the microdroplet increases as it passes the electrodes, and it becomes zero as it reaches the next electrode.

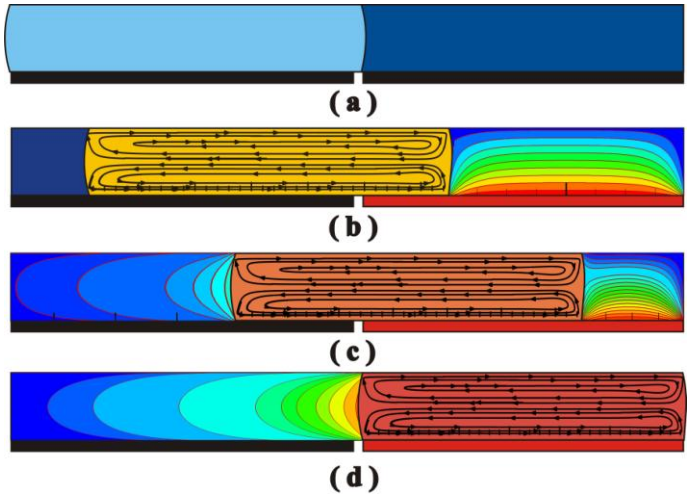

Figure 4: Solutions of hydrodynamics (inside) and electrostatics (outside) of the microdroplet for four different situations are shown: (a) time = 0 s shows the system under the condition of no applied voltage for which all the contact angles are 105^o, (b) time = 0.008 s, (c) time = 0.0123 s and (d) time = 0.02141 s.

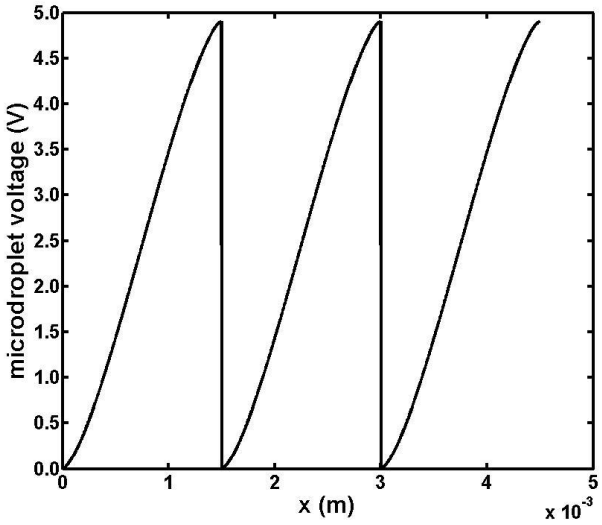

Figure 5: Microdroplet voltage as a function of its position is shown.

Figure 6 shows the advancing bottom, receding bottom and top contact angles of the microdroplet as a function of position, as it passes three electrodes. The change in the contact angle is due to the change of the microdroplet voltage as it passes the electrodes: The advancing bottom contact angle increases (from 101.9^o to 102.5^o) as the microdroplet passes each electrode due to the increase in the voltage (from 0V to 4.9V) inside the microdroplet (or the decrease in the voltage drop across the dialectic layer). Changes in the top contact angles (which are the same), follow a different trend as the contact angles decrease due to the increase of the voltage difference across the top layer. Since the bottom layer is thicker than the top layer,

the receding bottom contact angle does not change as much as the top contact angle (with the same voltage difference).

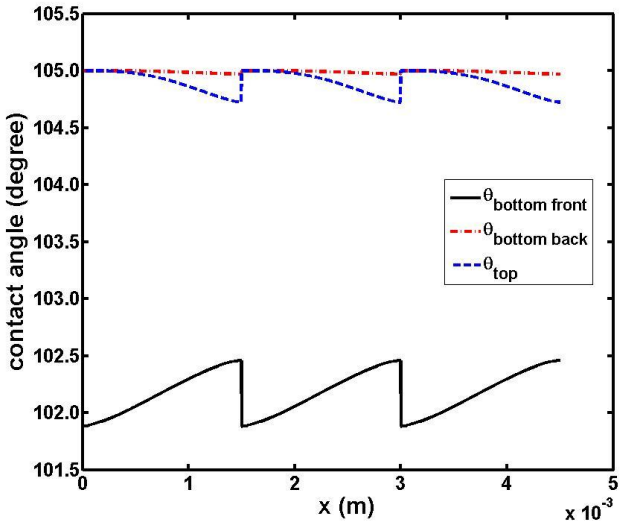

Figure 6: The advancing bottom, receding bottom and top contact angles of the microdroplet are shown as a function of its position.

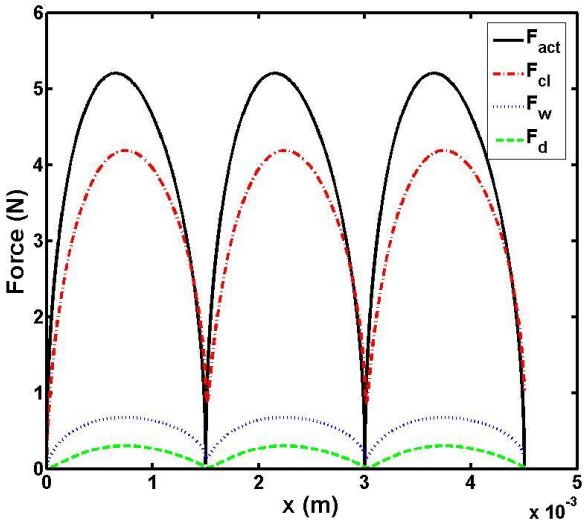

Figure 7: Actuation, contact line, drag and shear forces are shown as functions of microdroplet position.

It is known that the actuation force is a function of the microdroplet voltage. Thus, the actuation force changes as the microdroplet passes the electrodes. This change is shown in Figure 7. As can be seen here, the actuation force increases from zero to a maximum value and again reaches to zero as the advancing face of the microdroplet reaches the next electrode. The values of the forces (shown in Figure 7) are used to calculate the transient dynamics of the microdroplet. The result of the presented multiphysics modeling is shown in Figure 8. Equation (1) is solved, and the microdroplet motion is tracked. The transport frequency of the microdroplet is 50 Hz. The transient velocity of the microdroplet can also be found as a function of its position (see Figure 9). Jerky motion of the microdroplet motion is obvious here. The microdroplet starts its motion with zero velocity, and its velocity reaches to a maximum value (0.11 m/s). Interestingly, the velocity of the microdroplet due to its momentum does not reach to zero as it reaches to the next electrode.

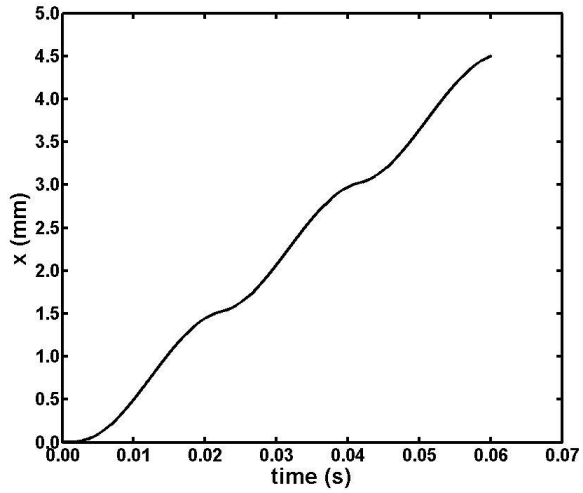

Figure 8: Location of the microdroplet as it is passing three electrodes is shown.

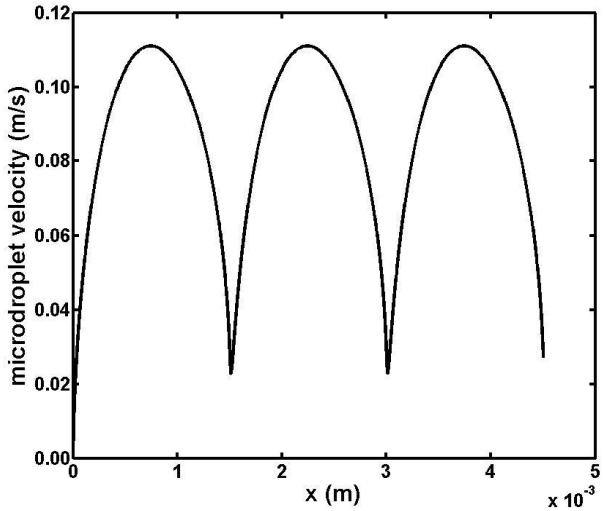

Figure 9: Transient velocity of the microdroplet is shown as a function of its position.

SUMMARY AND CONCLUSIONS

In this paper, the transient motion of microdroplets in digital microfluidic systems is modeled accurately. The developed model is based on coupling of hydrodynamic and electrostatic governing equations. Important findings of the proposed methodology include the transient velocity and location of the

microdroplet as well as the actuating and opposing forces acting on the microdroplet as functions of time. Moreover, the transport frequency of the microdroplet, being crucial in the design and control device processes, is found.

NOMENCLATURE

Symbol	Description	Units
$\vec{D}$	electric displacement vector	C/m²
D_x	*x*-component of electric displacement	C/m²
D_y	*y*-component of electric displacement	C/m²
d	microdroplet diameter	m
d^2x/dt^2	microdroplet acceleration	m/s^2
E	electric field	V/m
F_{act}	actuation force	N
F_w	wall force	N
F_d	drag force	N
F_{cl}	contact line force	N
h	gap spacing	m
L	electrode pitch	m
p_{hyd}	hydrodynamic pressure	Pa
p_{el}	electrostatic pressure	Pa
	Greek Symbols	
ε	permittivity of the filler	-
γ	liquid-vapor surface tension	N/m
Φ	electric potential	V

REFERENCES

[1] Pollack, M. G., Fair, R. B., Shenderov, A. D., 2000, "Electrowetting-based actuation of liquid droplets for microfluidic applications," Appl. Phys. Lett., 77, pp. 1725-1727.

[2] Lee, J., Moon, H., Fowler, J., Kim, C. J. and Schoellhammer, T., 2001, "Addressable micro liquid handling by electric control of surface tension," Proc. IEEE Int. Conf. MEMS, Interlaken, Switzerland, pp. 499-502.

[3] Abdelgawad, M., Wheeler, A. R., 2007, "Rapid prototyping in copper substrates for digital microfluidics," Adv. Mater., 19, pp. 133-137.

[4] Fair, R. B., 2007, "Digital microfluidics: is a true lab-on-a-chip possible?" Microfluid. Nanofluid., 3(3), pp. 245-281.

[5] Washizu, M., 1998, "Electrostatic actuation of liquid droplets for micro-reactorapplications," IEEE Trans. Ind. Appl., 34(4), pp. 732-737.

[6] Lee, J., Kim, C. J., 2000, "Surface-tension-driven microactuation based on continuous electrowetting," J. Microelectromech. Syst., 9(2), pp. 171-180.

[7] Bahadur, V., Garimella, S. V., 2008, "Energy minimization-based analysis of electrowetting for microelectronics cooling applications," Microelectron. J., 39(7), pp. 957-965.

[8] Bahadur, V., Garimella, S. V., 2006, "An energy-based model for electrowetting-induced droplet actuation," J. Micromech. Microengineering, 16(8), pp. 1494-1503.

[9] Baird, E., Young, P., Mohseni, K., 2007, "Electrostatic force calculation for an EWOD-actuated droplet," Microfluidics and Nanofluidics, 3(6), pp. 635-644.

[10] Ahmadi, A., Najjaran, H., Holzman, J. F., Hoorfar, M., 2009, "Two-dimensional flow dynamics in digital microfluidic systems," J. Micromech. Microeng., 19, pp. 065003-1-065003-7.

[11] Ren, H., Fair, R. B., Pollack, M. G., Shaughnessy, E. J., 2002, "Dynamics of electro-wetting droplet transport," Sens. Actuators B, 87(1), pp. 201-206.

[12] Gao, L., McCarthy, T. J., 2006, "Contact angle hysteresis explained," Langmuir, 22(14), pp. 6234-6237.

[13] Zeng, J., Korsmeyer, T., 2004, "Principles of droplet electrohydrodynamics for lab-on-a-chip," Lab on a Chip, 4(4), pp. 265-277.

[14] Jones, T. B., 2002, "On the relationship of dielectrophoresis and electrowetting," Langmuir, 18(11), pp. 4437-4443.

[15] Buehrle, J., Herminghaus, S., Mugele, F., 2003, "Interface profiles near three-phase contact lines in eectric fields," Phys. Rev. Lett., 91(8), pp. 86101.

[16] Ahmadi, A., Najjaran, H., Holzman, J. F., Hoorfar, M., 2009, "Determination of droplet shape in digital microfluidic systems using two-dimensional flow analysis," Proc. Nanotech, 3, pp. 351-354.

[17] Pollack, M. G., Shenderov, A. D., Fair, R. B., 2002, "Electrowetting-based actuation of droplets for integrated microfluidics," Lab on a Chip, 2(2), pp. 96-101.